The EMBO Journal vol.14 no.20 pp.4914–4921, 1995

The 3-D structure of a zinc metallo-β-lactamase from *Bacillus cereus* reveals a new type of protein fold

A.Carfi, S.Pares, E.Duée, M.Galleni[1], C.Duez[1], J.M.Frère[1] and O.Dideberg[2]

Institut de Biologie Structurale Jean-Pierre Ebel (CEA-CNRS), Laboratoire de Cristallographie Macromoléculaire, 41 Avenue des Martyrs, F-38027 Grenoble Cedex 1, France and [1]Université de Liège, Institut de Chimie (B6), Centre d'Ingénierie des Protéines, B-4000 Sart-Tilman, Liège 1, Belgium

[2]Corresponding author

The 3-D structure of *Bacillus cereus* (569/H/9) β-lactamase (EC 3.5.2.6), which catalyses the hydrolysis of nearly all β-lactams, has been solved at 2.5 Å resolution by the multiple isomorphous replacement method, with density modification and phase combination, from crystals of the native protein and of a specially designed mutant (T97C). The current model includes 212 of the 227 amino acid residues, the zinc ion and 10 water molecules. The protein is folded into a ββ sandwich with helices on each external face. To our knowledge, this fold has never been observed. An approximate internal molecular symmetry is found, with a 2-fold axis passing roughly through the zinc ion and suggesting a possible gene duplication. The active site is located at one edge of the ββ sandwich and near the N-terminal end of a helix. The zinc ion is coordinated by three histidine residues (86, 88 and 149) and a water molecule. A sequence comparison of the relevant metallo-β-lactamases, based on this protein structure, highlights a few well-conserved amino acid residues. The structure shows that most of these residues are in the active site. Among these, aspartic acid 90 and histidine 210 participate in a proposed catalytic mechanism for β-lactam hydrolysis.

Keywords: antibiotic/β-lactamase/metalloenzyme/penicillin resistance/X-ray structure

Introduction

Only a few years ago, metallo-β-lactamases were considered as mere biochemical curiosities, compared with their widespread active-site serine counterparts which are responsible for the resistance of a large number of pathogenic bacterial strains to penicillins and related antibiotics. At that time, only innocuous strains of *Bacillus cereus* were known to produce two very similar monomeric metallo-β-lactamases. The discovery of a third metallo-β-lactamase (Saino *et al.*, 1982; Bicknell *et al.*, 1985) produced by *Xanthomonas maltophilia*, composed of four subunits but devoid of allosteric properties, did not seem to raise major concerns in the medical community. However, the more recent finding that the resistance to carbapenems of an increasing number of clinically noxious strains is caused by the synthesis of Zn^{2+}-containing β-lactamases is a cause of concern (Payne, 1993).

Two major factors are responsible for the re-evaluation of the clinical importance of these enzymes. Firstly, they generally hydrolyse carbapenems (e.g. imipenem) with a high efficiency, while these compounds generally escape the activity of the active-site serine enzymes. Secondly, an identical or similar gene has been found in various strains of *Serratia*, *Pseudomonas* and *Enterobacter* (Yang *et al.*, 1990). Because this gene is probably plasmid-borne, and on the basis of previous experience, its spread to an ever increasing population of pathogenic species is now considered as a distinct threat to our ability to fight a variety of infectious bacteria.

All the presently sequenced Zn^{2+} β-lactamases (including the *X.maltophilia* monomer) exhibit sequence similarities (see below), and it is likely that they are homologous and share a common catalytic mechanism. They appear to form a unique family, distinct from the other metallopeptidases [e.g. thermolysin and carboxypeptidase A (CPA) families].

Enzymes produced by two strains of *B.cereus*, 569/H/9 and 5/B/6, often referred to as β-lactamase II (BCII), have already been studied extensively. The zinc BCII is considered as 'broad spectrum' because it hydrolyses a large number of penicillins and cephalosporins (Crompton and Waley, 1986; Felici *et al.*, 1993), and three histidine residues have been identified as the Zn^{2+} ligands (Baldwin *et al.*, 1978, 1979; Galdes *et al.*, 1980) with the possible participation of a cysteine residue (Davies and Abraham, 1974).

Preliminary crystallographic studies of the Cd^{2+} derivative (Sutton *et al.*, 1987) have confirmed these hypotheses, but the rather low resolution (3.5 Å) was not sufficient for proposing a complete chain tracing of the protein structure. Kinetic studies, sometimes performed at subzero temperatures and mainly with the Co^{2+} derivative, suggested the presence of various intermediates on the reaction pathway, none of them covalent (Bicknell *et al.*, 1986) but involving changes in the coordination sphere of the metal during catalysis (Waley, 1992).

Here, we describe the crystal structure of the *B.cereus* 569/H/9 enzyme at 2.5 Å resolution and propose a possible catalytic mechanism.

Results and discussion

Crystallization

Despite the recent progress in protein crystallography, some protein structures remain difficult to solve. Zn β-lactamases seem to belong to this group. For BCII, problems arise mainly from the lack of isomorphism of the heavy-atom derivatives to the native protein (Sutton *et al.*, 1987). To overcome this problem, recombinant

DNA technology was used. A mutant protein (T97C) was designed based on structural information from the low-resolution X-ray analysis (Sutton *et al.*, 1987). In principle, one or two sites for Hg binding are potentially accessible in the mutant protein depending on the size of the heavy-atom compound (the zinc site and regions near the newly introduced sulfydryl group).

Both proteins, the native and the T97C mutant, were crystallized in the same crystal form, close to that already published (Sutton *et al.*, 1987).

Quality of the model

The structure was solved by the multiple isomorphous replacement method, with density modification and phase combination, using X-ray data collected from the native protein and the T97C mutant derivative crystals. Refinement statistics are summarized in Table I. The current model consists of 212 of the 227 residues, one Zn^{2+} ion and 10 water molecules. The model has been refined to an *R*-factor of 22% using 6683 reflections [$|F| > 2\sigma(F)$] in the resolution range 8.0–2.5 Å. Two disordered chain segments could not be modelled: six residues (Ser1–Lys6) at the N-terminus and eight residues (Gly32–Val39) located between two β-strands.

All main-chain dihedral angles fall within the allowed regions of a Ramachandran plot (Ramachandran *et al.*, 1963), except those for Thr13 and Asp56 which were modelled with unfavourable dihedral angles of $\phi = 63.9°$, $\psi = 140.8°$ and $\phi = 72.8°$, $\psi = 139.7°$, respectively. The first of these residues (Thr13) is located in a loop region weakly defined in the electron density map; the second (Asp56) is buried in the protein, making a salt bridge with Arg91 in the groove of the enzymatic cavity.

Table I. Refinement data

	Number of reflections $\|F\| > 2\sigma$	*R*-factor[a] (%)
Resolution range 8.0–2.5 Å	6683	22.0
Protein atoms	1646	
Water molecules	10	
R.m.s. deviation from ideality		
Bond lengths (Å)	0.016	
Bond angles (°)	1.47	

[a]*R*-factor = $\Sigma|F_o - F_c|/\Sigma|F_o|$, where F_o and F_c are observed and calculated structure factor amplitude, respectively.

Overall structure of the Zn metallo-β-lactamase

A ribbon view of the 3-D structure of BCII is shown in Figure 1. BCII is a compact αββα protein of approximate dimensions 32×30×28 Å. The polypeptide chain is divided into two domains. These domains comprise strands and helices in the following order: $\beta_1\beta_2\beta_3\beta_4\beta_5\alpha_1\beta_6\alpha_2\beta_7\alpha_3$ and $\beta_8\beta_9\beta_{10}\beta_{11}\alpha_4\beta_{12}\alpha_5$ for the N- and C-terminal domains, respectively (Figure 2). α_2 has a kink caused by glycine residues 93 and 94. The core of the molecule is formed by two tightly packed β-sheets and is surrounded by five helices. Both β-sheets have the usual twist commonly observed in many proteins. Large loop regions connect some secondary structure elements. The two β-sheets can be superimposed, (β_2 to β_6) corresponding to (β_8 to β_{12}), by a 2-fold rotation. The result of the superposition is shown in Figure 3. The best fit of the two parts involves a rotation of exactly 180° without translation. For 58 equivalent C_α positions, we observed an r.m.s. deviation of 1.29 Å. Figure 3 shows many insertions and substantial deviations in helix positions. However, each domain contains the same set of topologically equivalent secondary structure elements, namely a βββββαβα motif. No significant sequence homology was found between the two motifs.

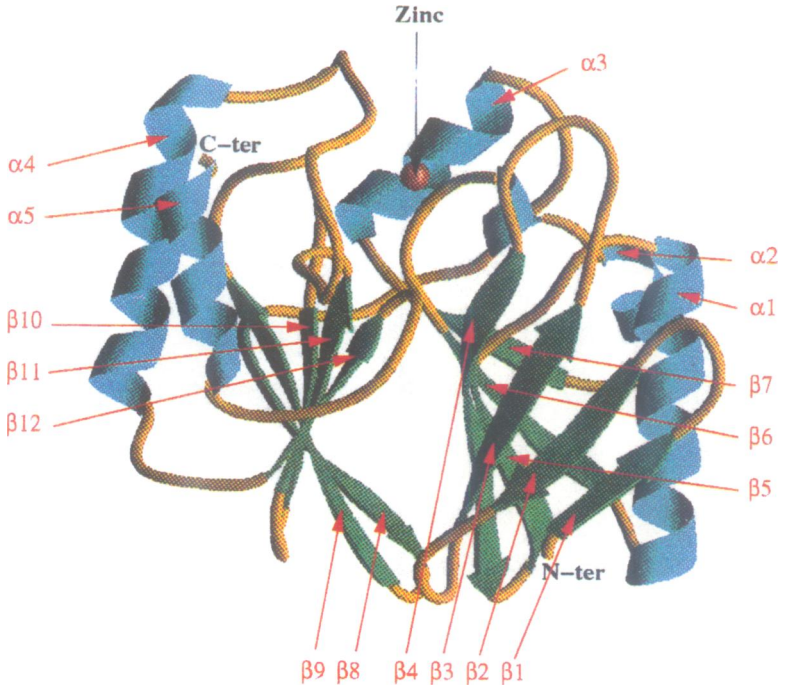

Fig. 1. Ribbon diagram of the molecular structure of *B.cereus* β-lactamase viewed roughly along the two β-sheets. The concave surfaces of the two sheets are the location of many hydrophobic residues. The zinc ion (in orange) is located at the edge between the two β-sheets.

The BCII structure has a ββ sandwich fold which is reminiscent of DNase I (Suck *et al.*, 1984; Oefner and Suck, 1986), the N-domain of glutamine 5-phosphoribosyl-1-pyrophosphate aminotransferase (Smith *et al.*, 1994), the multifunctional DNA repair enzyme exonuclease III (Mol *et al.*, 1995) and the proteasome subunits (Löwe *et al.*, 1995). However, the secondary structure elements forming the β-sheet are in a different order in BCII.

The observed αββα fold has no similarity with any known metalloprotein structure, including a D-alanine–D-alanine carboxypeptidase (Dideberg *et al.*, 1982) which cleaves the peptide bond between two D-alanine residues (the D-ala–D-ala moiety and penicillin are often considered isosteric).

Comparison with other Zn β-lactamases

All sequences were searched for in the EMBL Data Bank using FASTA (Lipman and Pearson, 1985) and aligned using the hydrophobic cluster analysis program (Gaboriaud *et al.*, 1987). Six sequences were considered first: *B.cereus* (569/H/9 and 5/B/6), *X.maltophilia*, *Bacteroides fragilis*, *Serratia marcescens* and *Aeromonas hydrophila*. Because the two *B.cereus* sequences differ by only 24 amino acid substitutions, only 569/H/9 was used for further analysis. When *B.cereus* (569/H/9) was compared with the other four sequences, sequence similarities ranged from 41 (*B.fragilis*) to 21% (*X.maltophilia*). While the other enzymes are monomeric, the *X.maltophilia* enzyme is a tetramer in the native state.

For alignment, the lengths of all secondary structure elements of the BCII structure were retained for the four other sequences. As seen in Figure 4, only a few deletions or insertions are required to align all the sequences. As expected, the main differences appear for *X.maltophilia*, with two large insertions between secondary structures: α_3 and β_8 (16 amino acids), and β_{10} and β_{11} (six amino acids). Finally, only nine amino acid residues are strictly conserved in the five sequences: Leu67, His88, Asp90, Gly93, Leu114, His149, Gly179, Asn180 and His210.

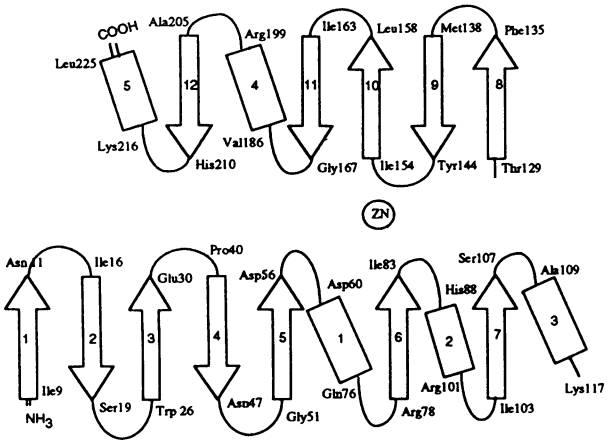

Fig. 2. BCII polypeptide topology of the two β-sheets. The β-strands are depicted as arrows, with the arrow heads indicating the direction of the chain. α-Helices are shown as rectangles.

Structure of the active site

The active site is located at the bottom of a groove running between the two β-sheets (Figure 1). The zinc ion is bound (Zn^{2+}···Nε or δ, ~2.2 Å) to three protein ligands (His86, His88 and His149). In the ligand sphere, a density was observed in a ($|F_o| - |F_c|$) map which, as for all known zinc metalloproteases, could be attributed to a water molecule (Wat1) or a hydroxyl ion. The four Zn^{2+} ligands are arranged in a distorted tetrahedral shape. The region of the ($2|F_o| - |F_c|$) electron density map around the zinc ion is shown in Figure 5. Seven out of the nine strictly conserved residues are located in the active site: His88, Asp90, Leu114, His149, Gly179, Asn180 and His210. Clearly, a hydrogen-bond network involving Zn^{2+}, Wat1, Asp90 and Cys168 is important for enzymatic activity.

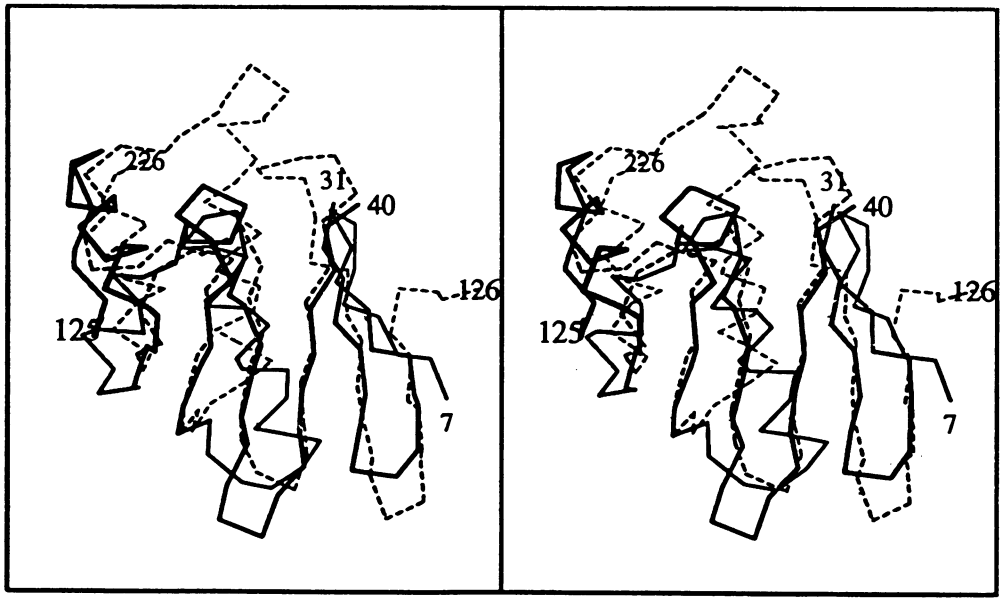

Fig. 3. Stereoview of the superposition of the C_α atoms of the two domains of the *B.cereus* β-lactamase. The N-terminal domain (7–105) and the C-terminal domain (126–226) are represented by continuous and dashed lines between C_α atoms, respectively.

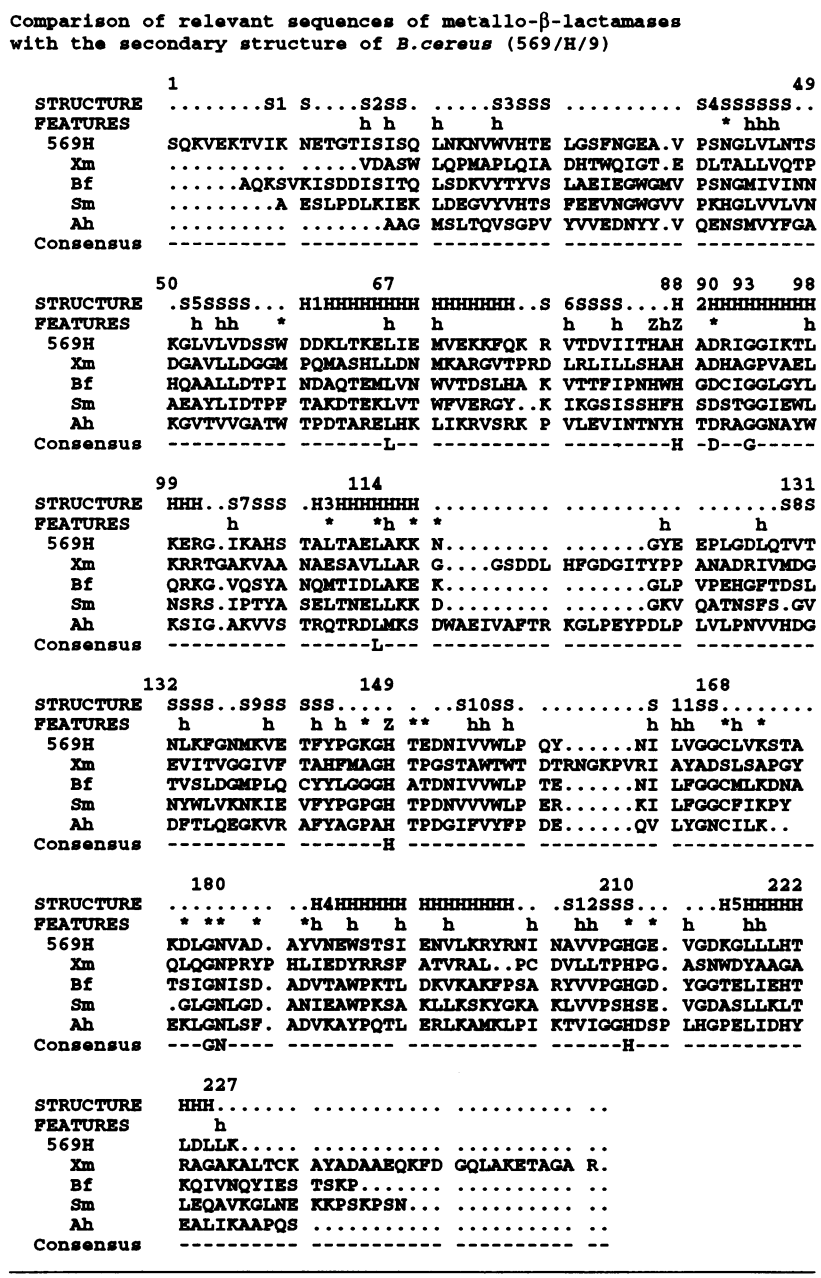

Fig. 4. Comparison of relevant sequences of metallo-β-lactamases with the secondary structures of *B.cereus* (569/H/9). Residues in the active site, zinc ion binding residues and conserved hydrophobic residues are marked with an '*', a 'Z' and an 'h', respectively. Structure codes: S, β-strand; H, α-helix. Sequences are: 569H, *B.cereus* (569/H/9) (Ambler *et al.*, 1985; Hussain *et al.*, 1985; Kato *et al.*, 1985); Xm, *X.maltophilia* (Walsh *et al.*, 1994); Bf, *B.fragilis* (Rasmussen *et al.*, 1990; Thompson and Malamy, 1990); Sm, *S.marcescens* (Osano *et al.*, 1994); Ah, *A.hydrophila* (Massida *et al.*, 1991).

NMR studies have suggested Cys168, which is replaced by a serine in *X.maltophilia*, as a potential fourth Zn^{2+} ligand (Galdes *et al.*, 1980), but the Zn^{2+}–S distance is 4.4 Å, too long for metal ion ligation. However, Cys168 interacts with Wat1, which is held in a correct position by three strong interactions: Zn^{2+}···Wat1 (3.0 Å), Cys168SG···Wat1 (2.9 Å) and Asp90OD2···Wat1 (2.6 Å). Leu114 makes van der Waals contacts with Ala87, located near two zinc ligands (His86 and His88). Finally, Gly179, Asn180 and His210 are too far from the active site to participate directly in the enzymatic mechanism, but they may be responsible for specific interactions with the β-lactam substrate (see below).

Mechanism of catalysis

The catalytic mechanism of zinc peptidases has been understood for some time. However, the exact role attributed to the Zn^{2+} ion has been altered slightly after the determination of the high-resolution structures of native proteins or tightly bound complexes. Today, after the pioneering work of Matthews (1988) on thermolysin and of Lipscomb (1983) on CPA, two superfamilies have been studied extensively: the thermolysin–metzincin family (Stöcker *et al.*, 1993, 1995; Hooper, 1994; references to the original work can be found in these three papers) and the carboxypeptidase family (Hooper, 1994). However, many other biochemical processes representing very

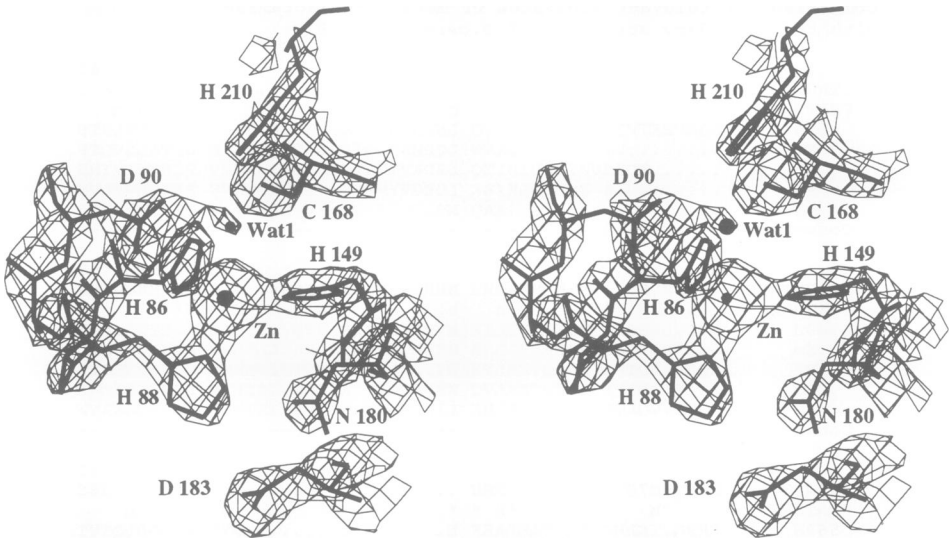

Fig. 5. View of the final ($2F_o - F_c$) electron density map around the Zn^{2+} ion, computed with calculated phases and contoured at 2σ above the mean.

diverse chemical reactions are also mediated by zinc catalysis (e.g. carbonic anhydrase, various dehydrogenases, adenosine deaminase).

In zinc peptidases, the metal ion has a dual role in catalysis. Firstly, the Zn^{2+}-bound water molecule is activated to perform a nucleophilic attack on the peptide carbonyl. Secondly, the Zn^{2+} binds and polarizes this carbonyl group. A negatively charged group, Glu143 in thermolysin and Glu270 in CPA, participates in the activation of the water molecule. After the water attack, a tetrahedral intermediate is formed, followed by the back delivery of a proton to the peptide nitrogen and the cleavage of the peptide bond.

Similar partners are present in BCII. A schematic diagram of the interaction with a substrate (Figure 7) was obtained by docking a cephalosporin molecule in the active site so that each partner was in an adequate position to act as mentioned above: $Zn^{2+}\cdots O_9$ (3.1 Å), $Wat1\cdots C_8$ (2.9 Å). Only one orientation of the cephalosporin can fit into the groove without colliding with protein atoms. Figures 6 and 7 suggest a reaction pathway in which the zinc ion activates Wat1 for nucleophilic attack with the participation of Asp90, acting as a general base to remove a proton from the water molecule. Both side chains, Asp90 and Cys168, maintain the water molecule in a position which allows the nucleophilic attack. A water proton is back delivered to N_5, and the C_8–N_5 bond is cleaved by a concerted mechanism. The simulated binding of cephalosporin (Figure 7) revealed two other interesting potential interactions: (i) the β-lactam carboxylate group makes an electrostatic interaction with His210, and (ii) the β-lactam side chain is near the loop containing Gly179 and Asn180. These three amino acids are strictly conserved in all Zn β-lactamase sequences. In support of the proposed mechanism, the substitution of residues Asp90 (Lim *et al.*, 1991), Cys168 and His210 (Clark, 1993) by site-directed mutagenesis resulted in severely impaired enzymes.

A preliminary comparison of the *B.cereus* Zn β-lactamase with CPA was made by superposing the active sites of CPA and BCII (Figure 8). Both enzymes interact with

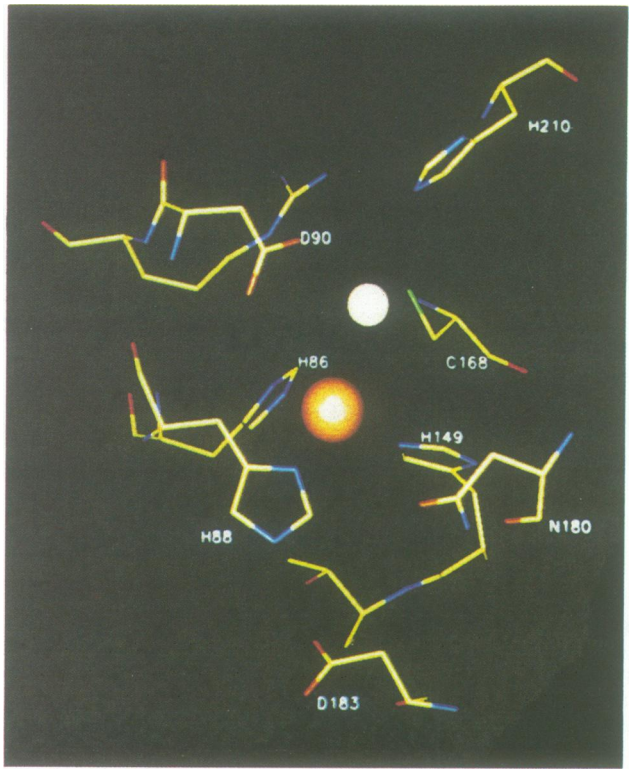

Fig. 6. View of the active site. The Zn^{2+} ion and the water molecule (Wat1) are represented by an orange and a white sphere, respectively.

a substrate bearing a carboxylate group. Because the two structures have different folds, the superposition was made in two steps: the two zinc ions were overlaid and then the three zinc ligands were superimposed. Among the three possible superpositions, that which brings the Glu270 of CPA near the Asp90 of BCII was selected. With this orientation, Arg145, which makes a salt bridge interaction with the carboxylate group of the substrate in CPA, is located near His210 of BCII. A more detailed comparison between *B.cereus* Zn β-lactamase and other Zn peptidases

must await the results of the further refinement of the BCII structure at high resolution.

Materials and methods

Site-directed mutagenesis

The procedures used in recombinant DNA techniques were essentially those described in Maniatis *et al.* (1982). The oligonucleotides were purchased from Eurogentec (Belgium). The site-directed mutagenesis was performed by inverse PCR (Clackson *et al.*, 1991) using the following strategy. A *Sst*II–*Pst*I (~650 bp) fragment comprising the triplet to be mutated was isolated from plasmid pRWH012 (Hussain *et al.*, 1985) and subcloned into plasmid pSL1180 (Pharmacia, LKB Biotechnology). The pair of primers was designed in inverted tail-to-tail directions: a 23 base primer (AATTCGATCAGCGTGCGCATGTG) annealing perfectly with the target sequence and a 28 base primer (GGCGGAATAAAATGTTTGAAAGAAAGAG) introducing three contiguous mismatches for replacing the ACG triplet in the coding sequence. The inverse PCR product was analysed by agarose gel electrophoresis and purified on an Ultrafree MC filter (Millipore). A fraction (one-sixth) of the purified product was then phosphorylated in 20 ml of DNA ligation buffer (Boehringer) using 5 U of T4 polynucleotide kinase for 30 min at 37°C. After heat denaturation of the kinase, ligation was performed by adding 1 U of T4 DNA ligase to the mixture and the product was used to transform RRI-competent cells. The presence of the desired mutation and the absence of any other unwanted mutation were checked by DNA sequencing using the CTGCAGTTAATGCTGTAC oligodeoxynucleotide (annealing 46 bases upstream of the mutated triplet) as a primer.

BCII expression in Escherichia coli

The *B.cereus* 569/H/9 and T97C mutant metallo-β-lactamases were produced in *E.coli* using the pRTWH012 plasmid cloned in *E.coli* DH1.

Purification of BCII and BCII (T97C)

A total of 20 l of Luria–Bertani medium were inoculated with 300 ml of an overnight culture of DH1/pRTWH012. After 10 h of growth under agitation at 37°C, the *E.coli* cells were harvested by centrifugation. The pellet was resuspended in 10 mM Tris, pH 8.0, buffer containing lysozyme (0.1 mg/ml). The solution was incubated for 30 min on ice. Following cell lysis by three cycles of freezing and thawing, the extract was centrifuged for 30 min at 30 000 *g*. The soluble fraction (which contains the β-lactamase) was submitted to ultrafiltration and an overnight dialysis against 10 mM cacodylate sodium, pH 6.5, buffer containing 50 μM $ZnSO_4$ (buffer A). The fraction was loaded onto a CM–Sepharose (55×3 cm) column (Pharmacia, Uppsala, Sweden) equilibrated with the same cacodylate buffer at a flow rate of 2.0 ml/min. The enzyme was eluted by a salt gradient (0.0–0.5 M NaCl). The active fractions were

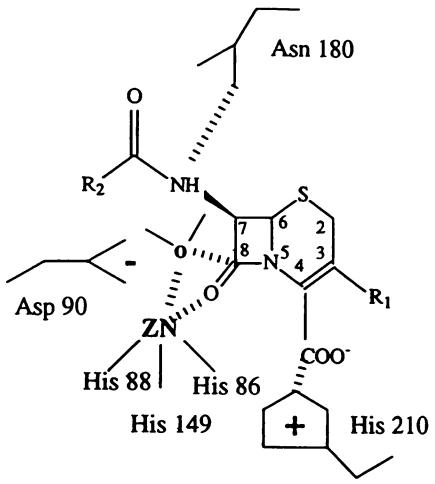

Fig. 7. Schematic diagram of the proposed interaction of a cephalosporin molecule prior to catalysis.

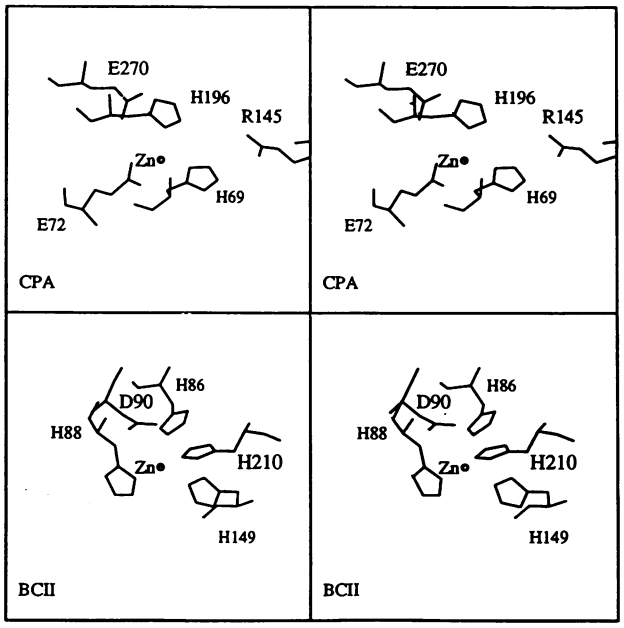

Fig. 8. Stereoview of the catalytic sites for selected amino acid residues around the Zn^{2+} ion for CPA (top) and BCII (bottom).

Table II. Crystallographic data

Data collection parameter	Crystal				
	1	2	3	4	5
Data set (protein)	(native)	$HgAc_2$ (native)	pHgAc (T97C)	pHgAc (T97C)	pCMBS (T97C)
Resolution (Å)	2.5	2.3	2.5	2.5	2.5
No. of reflections measured	11 206	20 937	31 281	17 070	15 819
R_{merge}[a]	0.030	0.036	0.047	0.052	0.040
No. of unique reflections	6911	9503	7942	7547	7776
Completeness (%)	86.0	90.6	98.2	93.9	96.0
R_{iso}	–	0.18	0.17	0.16	0.16
Phasing power[b]	–	1.42	1.81	1.95	1.31 (3.0 Å)
R_{Cullis} iso[c]	–	0.75	0.67	0.64	0.75
R_{Cullis} ano[c]	–	0.75	–	0.91	–
No. of sites	–	1 (Zn)	1	1	1

$HgAc_2$, mercuric acetate; pHgAc, phenylmercuric acetate; pCMBS, para-chloro-mercuribenzene sulfonic acid.
[a]R_{merge} of isomorphous data = $(\Sigma|I - \langle I\rangle|/\Sigma\langle I\rangle)$, where I is the measured intensity for each reflection and $\langle I\rangle$ is the mean intensity averaged from multiple observations of symmetry-related reflections.
[b]Phasing power = r.m.s. $(\langle F_H\rangle/E)$, where F_H is the heavy atom structure factor amplitude and E is the residual lack of closure.
[c]$R_{Cullis} = \Sigma||F_{PH}| - (|F_{PH}| - |F_P|)|/\Sigma|F_H|$, for centric reflections, where F_{PH} is the heavy-atom derivative structure factor.

pooled and concentrated by ultrafiltration. The sample was filtered through a Superdex™ 75 10/30 molecular sieve column (Pharmacia) pre-equilibrated with buffer A at a flow rate of 0.7 ml/min. The purity of the sample was estimated on the basis of the specific activity and by SDS–PAGE analysis and Coomassie Blue staining. The samples were analysed by electrospray mass spectroscopy. For this preparation, 60 mg of *B.cereus* 569H/9 β-lactamase were obtained. The enzyme (4 mg/ml) was stored in buffer A at –20°C. The purification of the T97C mutant was performed by the same procedure, but dithiothreitol (DTT; 50 μM) was added to the different buffers to prevent oxidation of the newly introduced cysteine.

Crystallization

Crystals of the wild-type protein (Table II, column 1) were grown by the vapour diffusion hanging drop method. The protein solution (9 mg/ml in 10 mM cacodylate buffer containing 100 μM $ZnSO_4$ and 50 μM DTT) was brought to 25 mM sodium citrate and 18% (w/v) poly(ethylene glycol) 8000 (PEG 8K) (Sigma), pH 5.6. For the T97C mutant protein, the DTT concentration was increased to 400 μM. For the preparation of mercuric acetate ($HgAc_2$) derivative (Table II, column 2), wild-type crystals were washed for 4 days in Zn^{2+}-free solutions containing 1.5 mM EDTA and 20% PEG 8K, and then soaked for 12 h in a 20% PEG and 300 mM Hg^{2+} solution. For derivatives of the mutant T97C, crystals were transferred to a DTT-free solution with 100 μM Zn^{2+}, 20% PEG 8K and either 0.35 mM phenylmercuric acetate (pHgAc) for 12 h or 0.5 mM pCMBS for 24 h. The second PMAc derivative (Table II, column 4) was prepared in solution by dialysing the protein solution for 5 h against a solution containing saturated pHgAc at pH 8.0 (50 mM Tris–HCl buffer) and then crystallized as the wild-type protein.

Data collection and processing

Crystals belonged to space group C2, with unit cell dimensions a = 53.79 Å, b = 61.98 Å, c = 69.97 Å, β = 93.67°, one molecule per asymmetric unit and a solvent content of 35%.

X-ray data for crystals reported in columns 1, 2, 4 and 5 of Table II were collected using a Fast/Enraf-Nonius area detector with a Cu rotating anode generator (FR5H) and a graphite monochromator, and were processed using the MADNES program (Messerschmidt and Pflugrath, 1987).

Data for the T97C mutant (Table II, column 3) were collected on a Mar-Research image plate detector using a Cu rotating anode generator (RU 200), and were processed with the XDS program (Kabsch, 1988, 1993). The CCP4 program suite (1993) was used for further processing.

Structure solution and refinement

The structure was solved by multiple isomorphous replacement (MIR). The mercury atom of the wild-type derivative (Table II, column 2) was found to replace the zinc atom. In the mutant T97C derivatives, the Hg atom was bound to the –SH group in slightly different positions for the pCMBS derivative and the two pHgAc derivatives. Heavy-atom parameter refinement and phasing were performed using MLPHARE (CCP4, 1993). The MIR map was improved by an electron density modification involving solvent flattening, histogram matching and Sayre's equations options of the dm program (CCP4, 1993). The resulting map was partially interpretable, and allowed ~60% of the protein atoms to be located. Successive cycles of phase combination with SIGMAA (Read, 1986) and model building resulted in the final model, which defines the protein structure except for the C-terminal Lys227 and two stretches of the sequence: the first six N-terminal residues and the Gly32–Val39 loop which appears to be disordered.

Model building was performed using the graphic O program (Jones *et al.*, 1991) on an ESV station. Refinement was performed using X-PLOR (Brünger, 1992) with 5% of the reflection data set used for defining the R-free factor. The correctness of the chain trace was verified by an inspection of the electron density of $(2|F_o| - |F_c|)$, $(|F_o| - |F_c|)$ and σ_A weighted $(|F_o| - |F_c|)$ omit maps calculated with ~10% of the residues omitted for the phase calculation.

The final model contains 212 amino acid residues (out of 227), one Zn atom and 10 water molecules which were clearly located in the map and refined with a B-factor of <50 Å^2. The final R-factor was 0.22 for the 6683 reflections with $|F| > 2\sigma(F)$ (0.221 for all 6709 reflections), and the R-free factor was 0.33 in the resolution range 8.0–2.5 Å.

Structure comparison

The structures were taken from the Protein Data Bank (Abola *et al.*, 1987). Figures were prepared using the following programs: MOLSCRIPT (Kraulis, 1991), RIBBONS (Carson, 1991) and O (Jones *et al.*, 1991).

Data deposition

The atomic coordinates have been deposited in the Protein Data Bank (1BMC), Chemistry Department, Brookhaven National Laboratory, Upton, NY 11973, with an embargo of 2 years after publication.

Acknowledgements

This is publication No. 276 of the Institut de Biologie Structurale Jean-Pierre Ebel. The authors would like to thank a number of people for their assistance: E.Forest and Y.Petillot (LSMP, Grenoble, France) for mass spectra analysis and P.Charlier (Liège, Belgium) for early crystallization trials. This work was supported by an ECC grant Human Capital and Mobility No. ERBCHRXCT930268, a French IMABIO program, an Action Concertée (convention 89/94-130) and the Belgian Government as part of a Pôle d'Attraction Interuniversitaire (PAI No. 19).

References

Abola,E.E., Bernstein,F.C., Bryant,S.H., Koetzle,T.F. and Weng,J. (1987) Protein data base. In Allen,F.H., Bergerhoff,G. and Sievers,R. (eds), *Crystallographic Databases — Information Content, Software Systems, Scientific Applications.* Data Commission of the International Union of Crystallography, Bonn, Germany, pp. 107–132.

Ambler,R.P., Daniel,M., Fleming,J., Hermoso,J.M., Pang,C. and Waley,S.G. (1985) The amino acid sequence of the zinc-requiring β-lactamase II from the bacterium *Bacillus cereus* 569. *FEBS Lett.*, **189**, 207–211.

Baldwin,G.S., Galdes,A., Hill,H.A.O., Smith,B.E., Waley,S.G. and Abraham,E.P. (1978) Histidine residues as zinc ligands in β-lactamase II. *Biochem. J.*, **175**, 441–447.

Baldwin,G.S., Waley,S.G. and Abraham,E.P. (1979) Identification of histidine residues that act as zinc ligands in β-lactamase II by differential tritium exchange. *Biochem. J.*, **179**, 459–463.

Bicknell,R., Emanuel,E., Gagnon,J. and Waley,S.G. (1985) The production and molecular properties of the zinc β-lactamase of *Pseudomonas maltophilia* II D 1275. *Biochem. J.*, **229**, 791–797.

Bicknell,R., Shaffer,A., Waley,S.G. and Auld,D.S. (1986) Changes in the coordination geometry of the active-site metal during catalysis of benzylpenicillin hydrolysis by *Bacillus cereus* β-lactamase II. *Biochemistry*, **25**, 7208–7215.

Brünger,A.T. (1992) *A System for X-ray Crystallography and NMR: XPLOR.* Version 3.0, Yale University Press, New Haven, CT.

Carson,M.C. (1991) RIBBONS 2.0. *J. Appl. Cryst.*, **24**, 958–961.

CCP4 (1993) Collaborative Computing Project No. 4. *Acta Crystallogr.*, **D50**, 760–763.

Clackson,T., Güssow,D. and Jones,P.T. (1991) In McPherson,M.J., Anirke,P. and Taylor,G.R. (eds), *PCR: A Practical Approach.* IRL Press, Oxford, UK, pp. 202–203.

Clark,S.D. (1993) Site directed mutagenesis of bacterial metallo-β-lactamase. PhD Thesis, Texas Technical University, TX.

Crompton,I.E. and Waley,S.G. (1986) The determination of specificity constants in enzyme-catalysed reactions. *Biochem. J.*, **239**, 221–224.

Davies,R.B. and Abraham,E.P. (1974) Metal cofactor requirement of β-lactamase II. *Biochem. J.*, **143**, 129–135.

Dideberg,O., Charlier,P., Dive,G., Joris,B., Frère,J.M. and Ghuysen,J.M. (1982) Structure of a Zn^{2+}-containing D-alanyl–D-alanine-cleaving carboxypeptidase at 2.5 Å resolution. *Nature*, **299**, 469–470.

Felici,A., Amicosante,G., Oratore,A., Strom,R., Ledent,P., Joris,B., Fanuel,L. and Frère,J.M. (1993) An overview of the kinetic parameters of class B β-lactamases. *Biochem. J.*, **291**, 151–155.

Gaboriaud,C., Bissery,V., Benchetit,T. and Mornon,J.P. (1987) Hydrophobic cluster analysis: an efficient new way to compare and analyse amino acid sequences. *FEBS Lett.*, **224**, 149–155.

Galdes,A., Hill,H.A.O., Baldwin,G.S., Waley,S.G. and Abraham,E.P. (1980) The ^{1}H nuclear-magnetic-resonance spectroscopy of Cobalt(II)-β-lactamase II. *Biochem. J.*, **187**, 789–795.

Hooper,N.M. (1994) Families of zinc metalloproteases. *FEBS Lett.*, **354**, 1–6.

Hussain,M., Carlino,A., Madonna,M.J. and Lampen,J.O. (1985) Cloning and sequencing of the metallothioprotein β-lactamase II gene of *Bacillus cereus* 569/H in *Escherichia coli*. *J. Bacteriol.*, **164**, 223–229.

Jones,T.A., Zou,J.Y., Cowan,S.W. and Kjeldgaard,M. (1991) Improved

methods for building protein models in electron density maps and the location of errors in these models. *Acta Crystallogr.*, **A47**, 110–119.
Kabsch,W. (1988) Evaluation of single X-ray diffraction data from a position sensitive detector. *J. Appl. Cryst.*, **21**, 916–924.
Kabsch,W. (1993) Automatic processing of rotation diffraction data from crystals of initially unknown symmery and cell constants. *J. Appl. Cryst.*, **26**, 795–800.
Kato,C., Kudo,T., Watanabe,K. and Horikoshi,K. (1985) Nucleotide sequence of the β-lactamase gene of alkalophilic *Bacillus* sp. strain 170. *J. Gen. Microbiol.*, **131**, 3317–3324.
Kraulis,P.J. (1991) MOLSCRIPT: a program to produce both detailed and schematic plots of protein. *J. Appl. Cryst.* **24**, 946–950.
Lim,H.M., Iyer,R.K. and Pene,J.J. (1991) Site-directed mutagenesis of dicarboxylic acids near the active site of *Bacillus cereus* 5/B/6 β-lactamase II. *Biochem. J.*, **276**, 401–404.
Lipman,D.J. and Pearson,W.R. (1985) Rapid and sensitive protein similarity searches. *Science*, **227**, 1435–1441.
Lipscomb,W.N. (1983) Structure and catalysis of enzymes. *Annu. Rev. Biochem.*, **52**, 17–34.
Löwe,J., Stock,D., Jap,B., Zwickl,P., Baumeister,W. and Huber,R. (1995) Crystal structure of the 20S proteasome from the archaeon *T. acidophilum* at 3.4 Å resolution. *Science*, **268**, 533–539.
Maniatis,T., Fritsh,E.F. and Sambrook,J. (1982) *Molecular Cloning: A Laboratory Manual*. Cold Spring Harbor Laboratory Press, Cold Spring Harbor, NY.
Massida,O., Rossolini,G.M. and Satta,G. (1991) The *Aeromonas hydrophila* A gene: molecular heterogeneity among class B metallo-β-lactamases. *J. Bacteriol.*, **173**, 4611–4617.
Matthews,B.W. (1988) Structural basis of the action of thermolysin and related zinc peptidases. *Acc. Chem. Res.*, **21**, 333–340.
Messerschmidt,A. and Pflugrath,J.W. (1987) Crystal orientation and X-ray pattern prediction routines for area-detector diffractometer systems in macromolecular crystallography. *J. Appl. Cryst.*, **20**, 306–315.
Mol,C.D., Kuo,C.-F., Thayer,M.M., Cunningham,R.P. and Tainer,J.A. (1995) Structure and function of the multifunctional DNA-repair enzyme exonuclease III. *Nature*, **374**, 381–386.
Oefner,C. and Suck,D. (1986) Crystallographic refinement and structure of DNase I at 2 Å resolution. *J. Mol. Biol.*, **192**, 605–632.
Osano,E., Arakawa,Y., Wacharotayankun,R., Ohta,M., Horii,T., Ito,H., Yoshimura,F. and Kato,N. (1994) Molecular characterization of an enterobacterial metallo-β-lactamase found in a clinical isolate of *Serratia marcescens* that shows imipenem resistance. *Antimicrob. Agents Chemother.*, **38**, 71–78.
Payne,D.J. (1993) Metallo-β-lactamase: a new therapeutic challenge. *J. Med. Microbiol.*, **39**, 93–99.
Ramachandran,G.N., Ramakrishnan,C. and Sasisekharan,V. (1963) Stereochemistry of polypeptide chain configurations. *J. Mol. Biol.*, **7**, 95–99.
Rasmussen,B.A., Gluzman,Y. and Tally,F.P. (1990) Cloning and sequencing of the class B β-lactamase gene (ccrA) from *Bacteroides fragilis* TAL3636. *Antimicrob. Agents Chemother.*, **34**, 1590–1592.
Read,R.J. (1986) Improved Fourier coefficients for maps using phases from partial structures with errors. *Acta Crystallogr.*, **A42**, 140–149.
Saino,Y., Kobayashi,F., Inoue,M. and Mitsuhashi,S. (1982) Purification and properties of inducible penicillin β-lactamase isolated from *Pseudomonas maltophilia*. *Antimicrob. Agents Chemother.*, **22**, 564–570.
Smith,J.L., Zaluzec,E.J., Wery,J.-P., Niu,L., Switzer,R.L., Zalkin,H. and Satow,Y. (1994) Structure of the allosteric regulatory enzyme of purine biosynthesis. *Science*, **264**, 1427–1433.
Stöcker,W., Gomis-Rüth,F.-X., Bode,W. and Zwilling,R. (1993) Implications of the three-dimensional structure of astacin for the structure and function of the astacin family of zinc-endopeptidases. *Eur. J. Biochem.*, **214**, 215–231.
Stöcker,W., Grams,F., Baumann,U., Reinemer,P., Gomis-Rüth,F.-X., McKay,D.B. and Bode,W. (1995) The metzincins — Topological and sequential relations between the astacins, adamalysins, serralysins, and matrixins (collagenases) define a superfamily of zinc-peptidases. *Protein Sci.*, **4**, 823–840.
Suck,D., Oefner,C. and Kabsch,W. (1984) Three-dimensional structure of bovine pancreatic DNase I at 2.5 Å resolution. *EMBO J.*, **3**, 2423–2430.
Sutton,B.J., Artymiuk,P.J., Cordero-Borboa,A.E., Little,C., Phillips,D.C. and Waley,S.G. (1987) An X-ray-crystallographic study of β-lactamase II from *Bacillus cereus* at 0.35 nm resolution. *Biochem. J.*, **248**, 181–188.
Thompson,J.S. and Malamy,M.H. (1990) Sequencing the gene of imipenem–cefoxitin-hydrolyzing enzyme (CfiA) from *Bacteroides fragilis* TAL2480 reveals strong similarity between CfiA and *Bacillus cereus* β-lactamase II. *J. Bacteriol.*, **172**, 2584–2593.
Waley,S.J. (1992) β-lactamase: mechanism of action. In Page,M. (ed.), *The Chemistry of β-Lactams*. Blackie Academic and Professional, Chapman and Hall, London, UK, pp. 198–228.
Walsh,T.R., Hall,L., Assinder,S.J., Nichols,W.W., Cartwright,S.J., MacGowan,A.P. and Bennett,P.M. (1994) Sequence analysis of the L1 metallo-β-lactamase from *Xanthomonas maltophilia*. *Biochim. Biophys. Acta*, **1218**, 199–201.
Yang,Y., Wu,P. and Livermore,D.M. (1990) Biochemical characterization of a β-lactamase that hydrolyses penems and carbapenems from two *Serratia marcescens* isolates. *Antimicrob. Agents Chemother.*, **34**, 755–758.

Received on May 16, 1995; revised on July 21, 1995